Solving the Sayre equation by simulated annealing

Yan Chen and Wu-Pei Su*

Department of Physics and Texas Center for Superconductivity, University of Houston, Houston, TX 77204, USA. Correspondence e-mail: wpsu@uh.edu

Simulated annealing is used to solve the Sayre equation formulated as a minimization problem. Trial calculations for structures containing up to 126 non-H equal atoms have been carried out. The residual as a function of the fictitious temperature always exhibits a sudden drop before the emergence of the correct structure at low temperature. This behavior casts doubt on the suitability of solving the Sayre equation by steepest-descent methods.

1. Introduction

Sayre's equation (Sayre, 1952) has played a prominent role in the development of direct methods. Most of the current methods of choice are, however, based on the tangent formula, which corresponds to only the phase part of the Sayre equation. There have been relatively few attempts to solve the Sayre equation directly for determining structures.

In this work, we seek to solve a system of Sayre equations by minimizing a residual formed from the equations. To avoid being trapped in local minima, simulated annealing is used for the minimization. It turns out that such an annealing procedure is essential for obtaining the correct structures. This insight discourages the use of steepest-descent methods for minimization.

To illustrate the points, we have carried out trial calculations involving two space groups, $P\bar{1}$ and $P2_12_12_1$. We used known structures and fabricated data. For $P\bar{1}$, we have been able to solve a structure containing 126 equal atoms. For $P2_12_12_1$, we have been limited to smaller structures because of computer time. The method is very straightforward and can be used as an an alternate direct method.

2. Methodology

The following is a system of Sayre equations:

$$F(\mathbf{h}) = [Kf(\mathbf{h})/g(\mathbf{h})] \sum_{\mathbf{k}} F(\mathbf{k})F(\mathbf{h} - \mathbf{k}), \qquad (1)$$

where $f(\mathbf{h})$ and $g(\mathbf{h})$ are the scattering factors for the normal and square-density atoms, respectively, and K is an overall scaling constant.

A simple residual for the above set of equations is

$$R = \sum_{\mathbf{h}} |F(\mathbf{h}) - K[f(\mathbf{h})/g(\mathbf{h})]G(\mathbf{h})|^2$$
$$G(\mathbf{h}) = \sum_{\mathbf{k}} F(\mathbf{k})F(\mathbf{h} - \mathbf{k}). \qquad (2)$$

Minimization of the residual (Debaerdemaeker *et al.*, 1985; Woolfson & Fan, 1995) with respect to the phases of the structure factors $F(\mathbf{k})$ leads to solution of the original set of equations in (1). Owing to the possible existence of false minima, the simulated-annealing algorithm (Kirkpatrick *et al.*, 1983) is employed for the minimization procedure. Although the summation in (2) may extend over all available reflections, it is sufficient to include only strong reflections. In general, K
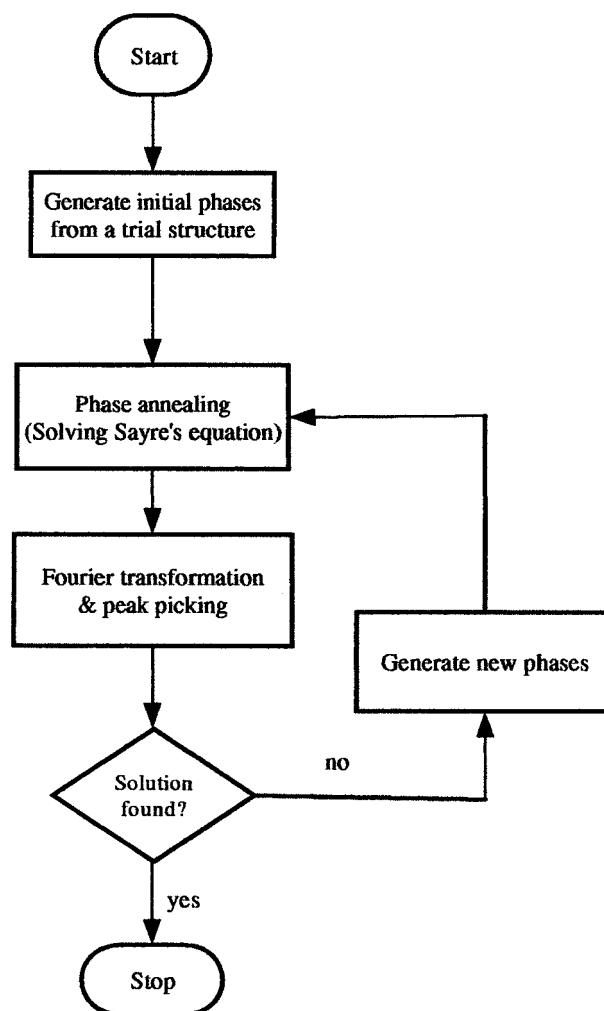

Figure 1
A flow chart of the phase-annealing procedure.

Table 1
Crystal data for the structures studied.

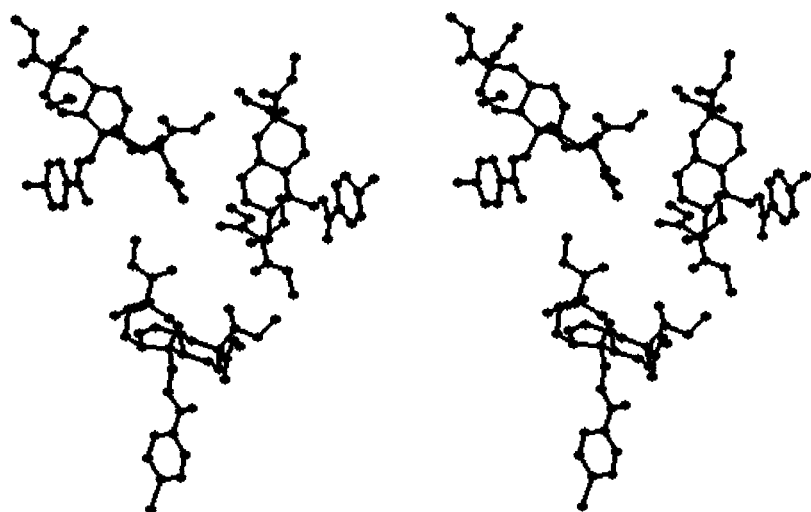|	Compound (1)	Compound (2)	Compound (3)	Compound (4)
Space group	$P\bar{1}$	$P\bar{1}$	$P\bar{1}$	$P2_12_12_1$
No. of non-H atoms	129	92	62	45
Cell setting	Triclinic	Triclinic	Triclinic	Orthorhombic
Z	2	2	2	4
a (Å)	13.549	12.533	8.221	10.749
b (Å)	15.413	12.649	16.245	13.068
c (Å)	24.490	25.319	17.337	22.643
α (°)	79.073	84.79	81.694	90
β (°)	75.749	80.74	89.656	90
γ (°)	70.254	83.84	86.468	90
Range of h,k,l	$-15 \rightarrow h \rightarrow 16$	$-13 \rightarrow h \rightarrow 13$	$-10 \rightarrow h \rightarrow 10$	$0 \rightarrow h \rightarrow 13$
	$0 \rightarrow k \rightarrow 18$	$-13 \rightarrow k \rightarrow 13$	$0 \rightarrow k \rightarrow 19$	$0 \rightarrow k \rightarrow 17$
	$-28 \rightarrow l \rightarrow 29$	$-20 \rightarrow l \rightarrow 27$	$-20 \rightarrow l \rightarrow 22$	$0 \rightarrow l \rightarrow 29$

Figure 2
Stereoview of the structure of compound (1).

in (2) should be treated as another variational parameter. To slightly simplify the calculations, we have preset K at the value that optimizes R for the correct structure. The results to be described below are not very sensitive to the value of K.

As in a typical simulated-annealing (Press *et al.*, 1992) procedure, one starts with a certain choice of the initial values of the phases at a high temperature. Specifically, in our algorithm, these phases are derived from a trial structure. A single phase is updated each time according to the Metropolis algorithm (Metropolis *et al.*, 1953). More precisely, the change in residual ΔR due to a move from the present value of the phase to another possible value is checked. If $\Delta R < 0$, then the move is accepted. If $\Delta R > 0$, the probability $\exp(-\Delta R/T)$ is compared with a random number ξ between 0 and 1: if $\xi < \exp(-\Delta R/T)$, the move is accepted, otherwise the phase retains its old value. This is similar to the update of atomic coordinates in a real-space approach (Su, 1995; Giacovazzo, 1998).

At any temperature T, each phase is updated a sufficient number of times to ensure thermal equilibrium. The temperature is decreased suffciently slowly (reduced by 10%

each step) so that hopefully the residual can reach its true minimum at the end of the annealing procedure. In any event, the result at the lowest temperature is examined by looking at the electron-density peaks derived from the phases to see if the structure makes sense or not. If it does not, one repeats the cycle by raising and lowering the temperature again. The starting phases of the new cycle are generated from the spatially filtered low-temperature configuration of the previous cycle. Many cycles may be needed for a sensible structure to emerge. A schematic flow diagram is depicted in Fig. 1.

In the following, we report on several trial calculations. The centrosymmetric structures are easier to solve because there are only two possible values for each phase, therefore it takes much less time to sample the phase configurations.

3. Examples

3.1. (*trans-syn-cis*)-Tetramethyl *rac*-(1*S*, 2*S*, 7*R*, 10*R*)-(8*Z*)-1-(4-bromobenzoyloxymethyl)tricyclo[8.5.0.0^{2,7}]pentadec-8-ene-5,5,13,13-tetracarboxylate ethanol solvate (3C$_{31}$H$_{37}$BrO$_{10}$ · 0.76C$_2$H$_6$O)

The original structure (Drouin *et al.*, 1997) (Fig. 2) contains 129 non-H atoms in the molecule (compound 1). We discard the heavy atoms, the remaining 126 non-H atoms are modeled by a Gaussian density $\exp[-(r/a)^2]$, where $a = 0.5$ Å. The unit-cell size and symmetry ($P\bar{1}$) are retained. Details of the crystal data are listed in Table 1. The 884 strongest independent reflections are picked from the synthetic data of 0.9 Å resolution. Although this data set is only a small fraction of the total number of reflections, it is sufficient to ensure that the correct structure does minimize the cost function.

For each temperature, we update the phases sequentially, *i.e.* from the first phase to the last phase (a single sweep). 40 sweeps per temperature are made. A typical plot of the residual *versus* temperature (the annealing curve) is shown in Fig. 3(*a*). The residual settles around 11 000 at low tempera-

ture. Examination of the low-temperature density configuration reveals no resemblance to the actual structure. After 50 cycles, a distinct annealing curve is spotted, as shown in
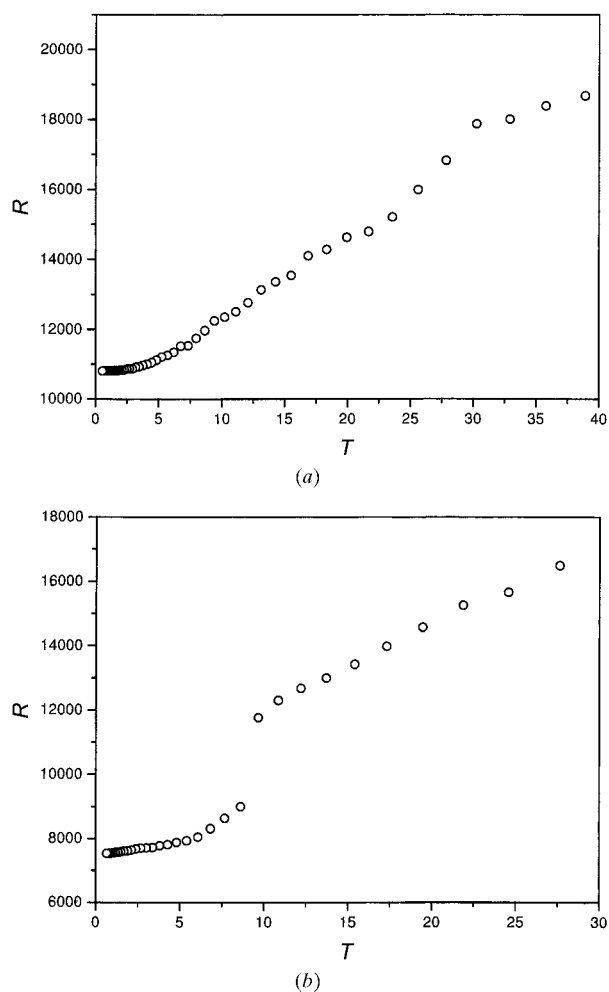

Figure 3
(a) A typical annealing (residual *versus* temperature) curve. (b) A distinct annealing curve giving rise to the correct structure studied in compound (1).
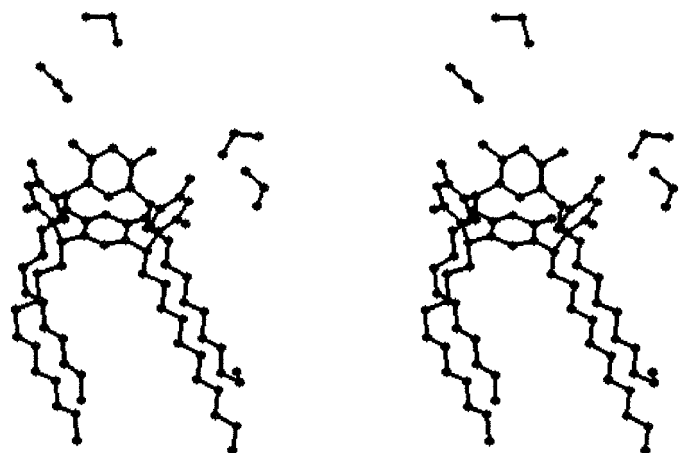
Fig. 3(b). A dramatic decrease of the residual at temperature T around 10 leads to a distinctly low residual (7500) and the correct structure.

The entire calculation above took about one week of CPU time on a Digital 500 MHz Alpha Workstation.

3.2. Alkyl calix[4]resorcinarene ($C_{72}H_{112}O_8 \cdot 4C_2H_6O$)

Again, we replace the actual structure (Hibbs *et al.*, 1998) by 92 identical Gaussians (compound 2) (Fig. 4). The space group is $P\bar{1}$. The 679 strongest independent reflections are used in the simulation. The structure emerges below temperature $T = 10$ after 40 cycles. The entire calculation took about two days on the same machine above.

3.3. Adduct of cyclam with 1,1,1-tris(4-hydroxyphenyl)-ethane methanol solvate ($2C_{20}H_{18}O_3 \cdot C_{10}H_{24}N_4 \cdot CH_4O$)

In the same fashion, we drop the H atoms and replace the C atoms, N atoms and O atoms in the original structure (Ferguson *et al.*, 1998) by identical Gaussians (compound 3). The unit cell shares the same space group and $Z = 2$ as in the above examples. 465 reflections are used. Eight cycles took a few hours and yielded the correct solution. To gain an insight into the nature of the phase-transition-like behavior of the annealing curve (Fig. 5), we examine some typical molecular configurations corresponding to the points Tb, Tm and Ta in Fig. 5. Each configuration is represented by the 124 highest peaks of the electron-density function in the unit cell with an interpeak separation larger than 0.6 Å. Configurations Tb and Tm are depicted by dots in Figs. 6(a) and 6(b), respectively. Configuration Ta is described by the wire frames in both figures. Apart from some minor defects (which disappear at temperatures below 2), configuration Ta is essentially indistinguishable from the native structure. Whereas there is a tendency for the dots to cluster around the correct structure in configuration Tb, many of them are locked into the final correct positions in configuration Tm. The above result is rather akin to the formation of a nucleation center above the melting temperature of an ordinary crystal. With that, the
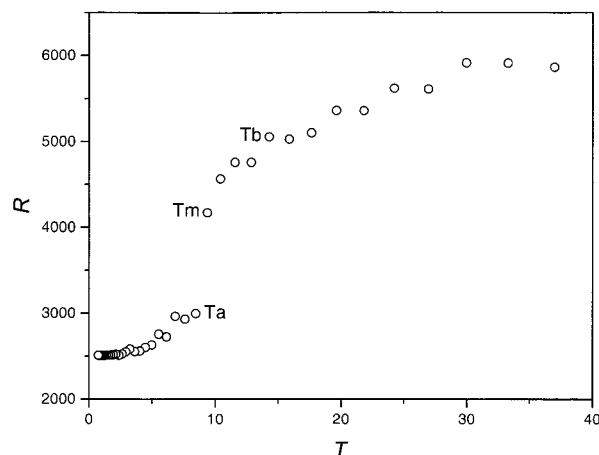

Figure 4
Stereodrawing of the molecular structure of compound (2).

Figure 5
An annealing curve of compound (3).

crystal develops quickly. Without that, the system could easily be trapped in a glassy metastable state as the temperature lowers.

3.4. Oxyacanthine ($C_{37}H_{40}N_2O_6$)

To find out how the algorithm works for other symmetry groups, we chose the oxyacanthine (Sivy *et al.*, 1996) molecule (Fig. 7) in the $P2_12_12_1$ space group with $Z = 4$ (compound 4). The higher symmetry requires longer summation in the calculation of the cost function. In addition, the phases can be continuous. To save time, we have discretized a continuous phase into integral multiples of $\pi/4$. 225 independent reflections are used. Each phase is updated 48 times at each temperature. The correct solution was found after 70 cycles, which took about ten days of CPU time. The annealing curve looks very similar to those in the previous examples.

4. Discussion

Since in most cases the presence of heavy atoms simplifies the solution of a structure, we have focused on light-atom structures in the test of a new method. The method we are proposing here is a very straightforward minimization procedure conceptually. In reality, one is limited by computer time as the structure gets larger or the symmetry becomes higher. This difficulty is related to the phase-transition-like behavior of the annealing procedure. Owing to that, the molecular configurational space needs to be sampled sufficiently extensively at appropriate temperatures so that a sharp drop in cost function can occur, ensuring the correctness of the final structure. We note here that a steepest-descent approach (Sayre, 1974) corresponds to quenching the system at zero temperature. According to our analysis of the thermodynamics of the annealing procedure, it seems unlikely such a quench could lead to the correct structure. The *SAYTAN* method (Debaerdemaeker *et al.*, 1985) also involves the minimization of R in (2) through the derivative of R with respect to the phases. As such, it might suffer from a similar problem of being trapped in a local minimum.

While simulated annealing is applied specifically to solving Sayre's equation in this paper, we note that it has been employed to solve the phase problem in other approaches. In a strictly real-space (Su, 1995) approach, it is used to minimize the discrepancy between calculated and observed intensities with respect to the atomic coordinates. Sheldrick (1990) has used it to fight the tendency of the tangent formula to produce overconsistent phase sets. Bhat (1990) has used it to improve the phases in a density-modification method. These are quite distinct applications. It seems that simulated annealing is slowly gaining popularity among researchers in X-ray crystallography.
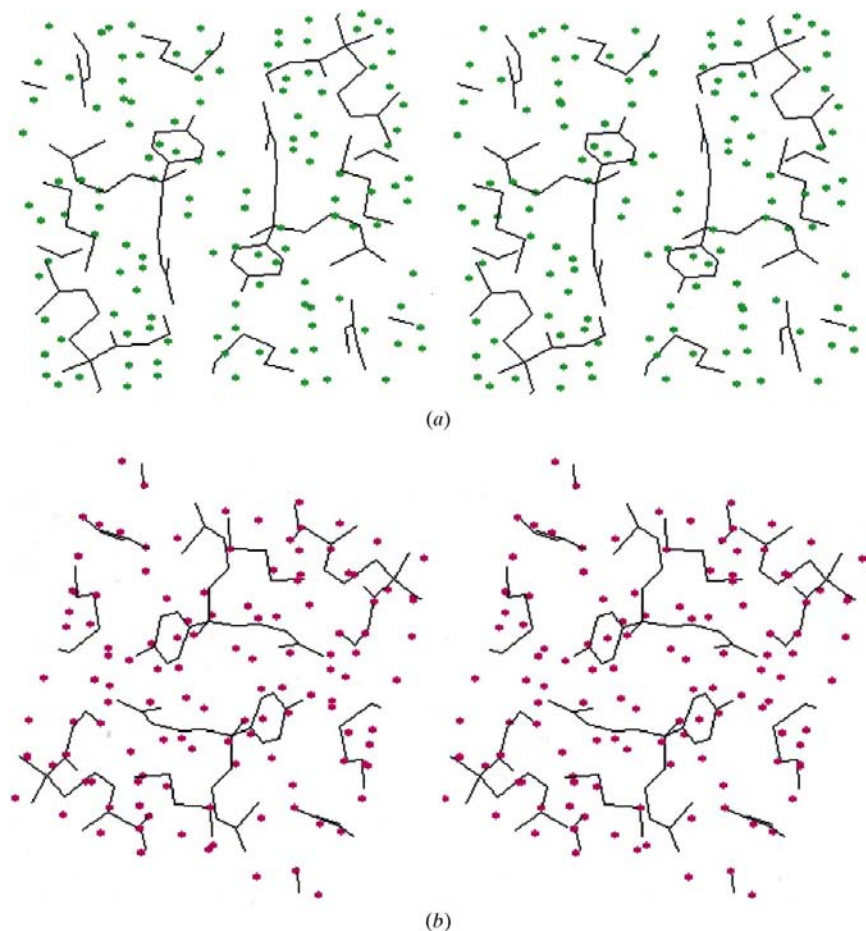
Figure 6
(*a*) Stereogram of configuration Tb superimposed on configuration Ta in wire frame. (*b*) Stereogram of configuration Tm superimposed on configuration Ta in wire frame.
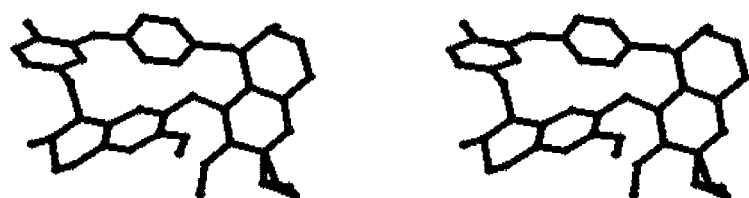
Figure 7
Stereograph of the molecular structure of oxyacanthine.

References

Bhat, T. N. (1990). *Acta Cryst.* A**46**, 735–742.

Debaerdemaeker, T., Tate, C. & Woolfson, M. M. (1985). *Acta Cryst.* A**41**, 286–290.

Drouin, M., Hall, D. G., Caille, A.-S. & Deslongchamps, P. (1997). *Acta Cryst.* C**53**, 1490–1493.

Ferguson, G., Glidewell, C., Gregson, R. M. & Meehan, P. R. (1998). *Acta Cryst.* B**54**, 139–150.

Giacovazzo, C. (1998). *Direct Phasing in Crystallography*, pp. 198–201. Oxford University Press.

Hibbs, D. E., Hursthouse, M. B., Abdul Malik, K. M., Adams, H., Stirling, C. J. M. & Davis, F. (1998). *Acta Cryst.* C**54**, 987–992.

Kirkpatrick, S., Gelatt, C. D. Jr & Vecchi, M. P. (1983). *Science*, **220**, 671–680.

Metropolis, N., Rosenbluth, A., Rosenbluth, M., Teller, A. & Teller, E. (1953). *J. Chem. Phys.* **21**, 1087–1092.

Press, W. H., Teukolsky, S. A., Vetterling, W. T. & Flannery, B. P. (1992). *Numerical Recipes: the Art of Scientific Computing*, pp. 436–448. Cambridge University Press.

Sayre, D. (1952). *Acta Cryst.* **5**, 60–65.

Sayre, D. (1974). *Acta Cryst.* A**30**, 180–184.

Sheldrick, G. M. (1990). *Acta Cryst.* A**46**, 467–473.

Sivy, J., Kettmann, V., Kostalova, D. & Vrabel, V. (1996). *Acta Cryst.* C**52**, 1479–1482.

Su, W.-P. (1995). *Acta Cryst.* A**51**, 845–849.

Woolfson, M. M. & Fan, H.-F (1995). *Physical and Non-physical Methods of Solving Crystal Structures.* Cambridge University Press.